Environmental Science
Water Research & Technology

ROYAL SOCIETY OF CHEMISTRY

PAPER

View Article Online
View Journal | View Issue

Cite this: *Environ. Sci.: Water Res. Technol.*, 2022, **8**, 2373

Superhydrophobic nanoparticle-coated PVDF–HFP membranes with enhanced flux, anti-fouling and anti-wetting performance for direct contact membrane distillation-based desalination

Ioannis Tournis, *[ab] Dimitris Tsiourvas, [b] Zili Sideratou, [b] Lamprini G. Boutsika,[b] Aggeliki Papavasiliou,[b] Nikos K. Boukos [b] and Andreas A. Sapalidis *[b]

Water is one of the most precious natural resources of the planet. Global water demand is expected to increase by 20–30% in near future, mainly due to the increase of industrial activities and domestic use. In this context, up to now, many water treatment technologies have been proposed to address water scarcity. Among them, processes based on membrane technology such as membrane distillation (MD) have received significant scientific and technological attention. In the present work, innovative nanocomposite polymeric membranes were developed, aiming to enhance the performance in relation to the state of the art membranes for desalination using direct contact membrane distillation (DCMD). To this aim, the development of porous poly(vinylidene fluoride-*co*-hexafluoropropylene) (PVDF–HFP) membranes and their modification by introducing a top layer of superhydrophobic fluorinated silicon nanoparticles on their surface was thoroughly studied. The developed membranes were characterized by a variety of techniques such as SEM, contact angle and liquid entry pressure (LEP). The superhydrophobic nanoparticle-coated membranes compared to pristine PVDF–HFP membranes, have improved fouling resistance properties, increased permeability and wetting resistance against various low surface tension organic compounds. The results indicate that the nanocomposite membranes exhibit improved overall performance aiming to tackle critical issues of membrane distillation process.

Received 31st May 2022,
Accepted 2nd August 2022

DOI: 10.1039/d2ew00407k

rsc.li/es-water

Water impact

Membrane distillation (MD) is an alternative water treatment technology for clean water recovery. Innovative nanocomposite membranes with enhanced wetting resistance and antifouling properties were prepared and studied, aiming to increase their permeate flux and lifespan. This work contributes towards optimised MD applications for the potential treatment of various waste waters with improved permeate water quality.

1. Introduction

Across the world, the demand for water will continue to rise. In particular, the water shortage increases due to various factors such as world's population growth, climate change and water pollution. One way to face this issue is through membrane-based water treatment, *e.g.* reverse osmosis (RO), which tends to be established as the main technology not only for brackish and seawater desalination, but also for the treatment of various wastes in order to recover purified water.[1,2]

Membrane distillation (MD) is a fairly new concept that is steadily gaining popularity in the field of desalination research as it combines the established desalination methods of membrane filtration and heating. The most common configuration of MD is direct contact membrane distillation (DCMD) in which the surfaces of the membrane are in direct contact with both heated feed and cold permeate fluids. The evaporation takes place at the hot feed-membrane side producing the vapor, which diffuses through the membrane and condenses at the surface-cold permeate side.[3,4] Although MD lacks in energy performance in comparison to reverse osmosis, there are instances where it is favorable to be used, such us for high salinity feedwaters (>50.000 TDS) and/or where waste or solar heat is abundantly available.[5,6]

The most common types of hydrophobic membranes used for MD application are made from polymers such as polyvinylidene fluoride (PVDF), polypropylene (PP) and

[a] *Department of Chemistry, National and Kapodistrian University of Athens, Zografou GR-15771, Greece*
[b] *Institute of Nanoscience and Nanotechnology (INN), NCSR "DEMOKRITOS", Agia Paraskevi, Attiki, GR-15341, Greece. E-mail: i.tournis@inn.demokritos.gr, a.sapalidis@inn.demokritos.gr*

polytetrafluoroethylene (PTFE). The most widespread technique of producing polymeric membranes is phase inversion which is defined as a demixing process where the initially homogeneous polymer solution is transformed, in a controlled way, from a liquid to a solid phase. The solidification process begins with the transition of a single liquid to two liquids (liquid–liquid demixing).[7,8] The liquid with the highest concentration of polymer will solidify to form the solid matrix while the low concentration region is responsible for the pore structure development.

In the last decades, efforts have been focused on the enhancement of the hydrophobicity of the membranes (water contact angle higher than 90°) or, even more, attempts have been performed to render them superhydrophobic (contact angle higher than 150°), which also results in an increase in permeability. In specific, Efome *et al.*[9] prepared flat sheet nanocomposite PVDF membranes containing superhydrophobic SiO_2 nanoparticles by the phase inversion technique and investigated their performance in vacuum membrane distillation. It was found that the maximum flux was observed at a nanoparticle concentration of 7 wt% with an average flux of around 3 kg m^{-2} h^{-1}, which was 4 times higher than that of the neat PVDF membrane. A salt rejection of more than 99.98% indicates that the fabricated membrane is suitable for vacuum membrane distillation. Additionally, Zhang *et al.*[10] developed a PVDF composite membrane with omniphobic property, where silica nanoparticles and PVDF microspheres were deposited on the PVDF membrane with the aid of polydopamine, followed by fluorosilanization of the modified membrane surface. The composite membrane presented superhydrophobicity with water contact angle (WCA) of 169.0° and oleophobicity with oil contact angle (OCA) of 112.1°. This study suggests that the re-entrant and anti-fouling PVDF composite membrane with omniphobic properties could be potentially applied in membrane distillation. In another work, Zheng *et al.*[11] prepared multiscale nano/microspheres (SiNPs@PS) based on electrostatic interactions between silica (SiNPs) and polystyrene (PS) microspheres, which subsequently were immobilized on the surface of a commercial PVDF porous membrane, followed by surface fluorination in order to obtain an omniphobic (both hydrophobic and oleophobic) membrane with hierarchical structure. This membrane mimicking the lotus surface due to its omniphobic character coupled with its excellent anti-fouling/anti-wetting properties was proposed to be used in DCMD treatment of oily emulsions.

In the present study, macroporous hydrophobic nanocomposite PVDF–HFP membranes having a superhydrophobic coating of fluorinated silicon nanoparticles (SiF-NPs) on their surface were produced following a simple and easily applicable method for membrane distillation-based desalination processes. The hydrophobic porous membranes were prepared by the phase inversion precipitation method using deionised water as the nonsolvent and acetone as solvent. A top layer of fluorinated silica nanoparticles was then applied using spin coating. Characterization was performed by means of scanning electron microscopy (SEM), liquid entry pressure of water (LEP_w) and contact angle. The membranes were also evaluated regarding their anti-fouling properties using protein adsorption tests, while their wetting resistance was assessed using different surface tension liquids. Finally, the membranes were tested in DCMD with NaCl solution and their performance was evaluated.

2. Experimental

2.1 Materials

Poly(vinylidene fluoride-*co*-hexafluoropropylene), PVDF–HFP, (average Mw ~ 455 000, Mn ~ 110 000), and acetone (ACS reagent, >99.5%) were purchased from Sigma-Aldrich (Merck KGaA, Darmstadt, Germany). Deionized (DI) water (conductivity <10 μS cm^{-1}) was used in all cases.

Tetramethyl orthosilicate (98%), 1*H*,1*H*,2*H*,2*H*-perfluorooctyltriethoxysilane (98%) and bovine serum albumin (BSA) were obtained from Sigma-Aldrich (Poole, UK). Hyperbranched polyethyleneimine (BASF, Lupasol G100, Mn ~ 5000) was kindly donated from BASF (Ludwigshafen, Germany).

2.2 Synthesis and characterization of fluorinated silicon oxide nanoparticles (SiF-NPs)

Previous studies have shown that silicon oxide (SiO_2) nanoparticles can be easily prepared employing a silicification process in water, under normal conditions with respect to temperature and pH, by allowing the condensation of silicic acid in the presence of minimum amounts of positively charged hyperbranched poly(ethyleneimine), adopting a method that is mimicking the formation of biosilica structures in nature.[12] The same principle was employed for the development of fluorinated silica nanoparticles as described in our previous publication (Scheme 1).[13] In short, 1 mL of a solution containing 1 M of silicic acid (obtained from the hydrolysis of tetramethyl orthosilicate in the presence of 1 mM HCl) and 0.3 M perfluorooctyltriethoxysilane was added in 10 mL of a 20 mM hyperbranched poly(ethyleneimine) solution in phosphate buffer (pH 7.5). The solution was allowed under stirring for 5 min, and the resulting nanoparticles were obtained after centrifugation (10 min, 12 000 RCF) and after repeatedly washing to remove any starting materials.

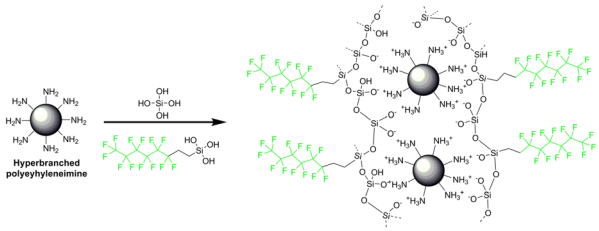

Scheme 1

2.3 Membrane preparation

PVDF–HFP was dissolved in acetone at 40 °C to prepare a 5% wt% stock solution. Deionized water (2 wt%) was added into the above solution under agitation, until the solution became homogeneous. After 1 h of stirring, the solution was cast in glass petri dish (diameter 12 cm) and left to dry in ambient conditions (22 °C and 40% r.h.) resulting in a porous structure obtained *via* vapor induced phase separation (VIPS). After evaporation (approximately 24 h), the resulting opaque membranes with thickness 60–65 μm were obtained.[14] The SiF-NPs were introduced on the surface of the prepared membranes by spin coating of an ethanol dispersion of SiF-NPs. The samples were span for 180 s at room temperature at a spin speed of 2000 rpm.

2.4 Characterization & performance evaluation

SEM images were obtained by a Jeol JSM 7401 F Field Emission Scanning Electron Microscope with Gentle Beam mode. EDX analysis of SiF-NPs was performed on a JEOL JXA 733 (AXES UA) (JEOL Ltd., Tokyo, Japan). For membrane cross-section imaging, the membrane was freeze-fractured in liquid nitrogen and then sputter-coated (Hitachi® E1020) with gold at an argon pressure of 13.3322 Pa (0.1 Torr) for 2 min at a current of 10 mA.

A Veeco Innova microscope coupled with Bruker RTESTPA-300 probes operating in non-contact (tapping) mode was employed for AFM imaging. The images were analyzed using the software Gwyddion.

The morphology of SiF-NPs was also investigated employing a FEI CM20 TEM microscope.

TGA measurements were collected on approximately 8 mg of each sample using a SETARAM SETSYS Evolution 18 Analyser, in the range of 35–800 °C, and at a heating rate of 10 °C min^{-1}, in an Al_2O_3 crucible under argon flow (30 mL min^{-1}).

Contact angle measurements using the sessile drop method were carried out at room temperature using a Kruss DSA-30 drop shape analyser. A 4 μL droplet of liquid was allowed to settle on the membrane surface and the digital image was acquired and processed to determine the contact angle. The liquids employed were octane, dodecane, methylnaphthalene, diidomethane and water. To minimize the experimental errors, the contact angles were measured at five random locations for each sample and then the average was reported. Surface energy (SFE) and work of adhesion (W_{ad}) were calculated by using the Geometrical Mean Model,[15] which is based on the contributions of two components, the dispersive (γ^d) and the polar (γ^p) as well as the Young Dupre' equation,[16] as follows:

$$SFE = \gamma^d + \gamma^p \quad (1)$$

$$SFE = \gamma_S + \gamma_L - 2\left(\sqrt{\gamma_s^d \cdot \gamma_L^d} + \sqrt{\gamma_s^p \gamma_l^p}\right) \quad (2)$$

which combined with the Young equation results in:

$$\gamma_L(1 + \cos\theta) = 2\left(\sqrt{\gamma_S^d \cdot \gamma_L^d} + \sqrt{\gamma_s^p \gamma_l^p}\right) \quad (3)$$

$$\text{and } W_{ad} = SFE(1 + \cos\theta) \quad (4)$$

An important property of any candidate MD porous membrane is the liquid entry pressure (LEP) value, which is desired to be as high as possible to prevent wetting of the membrane pores. This critical pressure difference is related to the surface tension of the fluid γ_L (N m^{-1}), the maximum pore radius r_{max} (m), the fluid contact angle θ (°) and assumes an intrinsic parameter for the pores' geometry B (—).[17] The calculation of this parameter is based on Franken equation, which for parameter $B = 1$ becomes equivalent to Young–Laplace's. In this case, takes the following form:

$$LEP = \frac{-2\gamma_L \cos\theta}{r_{max}} \quad (5)$$

The LEP was recorded as the pressure corresponding to the point of initial passage of water flow through the membrane.[18]

The porosity (ε) was determined by the gravimetric method, as defined in the following equation:[19]

$$\varepsilon = \left(\frac{w_{e+p} - \frac{w_p}{p_e}}{\frac{(w_{e+p} - w_p)}{p_e + \frac{w_p}{p_p}}}\right) \quad (6)$$

where, w_p, p_p (1770 kg m^{-3}) and w_e, p_e (786 kg m^{-3}) are the mass and density of sample and isopropanol, respectively.

Average pore radius (r_m), was calculated by filtration velocity method, measuring the water flux of the pristine and modified membrane in limited time under a specified pressure, respectevily. According to the following revised form of Guerout–Elford–Ferry equation[20] the average pore radius is:

$$r_m = \left(8(2.9 - 1.75\varepsilon)\frac{\eta\delta Q}{\varepsilon PA}\right)^{1/2} \quad (7)$$

where η is water viscosity (8.9×10^{-9} bar s), δ the membrane thickness (m), Q the flux per unit time (kg m^{-2} s^{-1}), P the operational pressure (bar) and A the effective membrane area (m^{-2}).

The membrane module for DCMD process consisted of two chambers, one for the feed and the other for the distillate, having an effective membrane area of 7×10^{-4} m^2. A 35 g L^{-1} aqueous NaCl solution was heated at 70 °C and fed in the module at a flow rate of 50 mL min^{-1}, while the permeate side was fed with ultrapure water (4.8 μS cm^{-1}) at a flow rate 40 mL min^{-1} and at a constant temperature of 17 °C assuring that the transmembrane pressure was kept below 20 mbar at all times. The flow rates were recorded electronically using Bronkhorst CORI-FLOW™ series mass flow meters. Yokogawa model ISC40G conductivity meters were recording the conductivities of feed and permeate side directly during the process. The temperature of both feeds was measured upstream from the membrane with a handheld temperature probe, Ω-Omega. The transmembrane pressure was recorded employing a Yokogawa model EJA110E differential pressure transmitter. Each

experiment lasted 4 h and the flux and rejection were taken as the average value under steady conditions. The permeate flux J (L m^{-2} h^{-1}) was calculated by the following equation:

$$J = \frac{U_p}{A_m} \quad (8)$$

where, U_P is the volumetric flow rate of vapor permeate, (L h^{-1}) and A_m is the effective membrane area, (m^2).

Salt rejection rate was calculated using the following equation:

$$R = \left(1 - \frac{C_p}{C_f}\right) \times 100\% \quad (9)$$

where, R is the percentage of the solute rejection, C_p is the concentration of the solute in the permeate and C_f is the concentration of the solute in the feed.

In DCMD, the mass transfer resistance[21] (B_m) can be described by assuming a linear relationship between the mass flux (J) and the water vapour pressure difference through the membrane:

$$J = B_m(p_{mf} - p_{mp}) \quad (10)$$

where p_{mf} and p_{mp} are the partial pressures of water at feed and permeate sides evaluated by using Raoult's law[22] at the temperatures T_{mf} and T_{mp}, respectively, such as the following:

$$p_{solution} = x_{solvent} \times p^{\circ}_{solvent}$$

It can be assumed that the mass transport takes place *via* the combined Knudsen/molecular-diffusion mechanism and the following equation is used to determine the mass transfer coefficient[23] (B^c_m):

$$B^c_m = \{3/2 \times \tau\delta/\varepsilon r \times (\pi RT/8M) + \tau\delta/\varepsilon \times P_a/PD \times RT/M\}^{-1} \quad (11)$$

where ε, τ, r and δ are the porosity (%), pore tortuosity, pore radius (nm) and thickness (μm) of the membrane, respectively, and M, R, T and P_a are the molar mass of water, gas constant (J mol^{-1} K^{-1}), absolute temperature (K) and air pressure (Pa), respectively. The value of PD (Pa m^2 s^{-1}) for water–air was calculated from the following expression:

$$PD = 1.895 \times 10^{-5} T^{2.072} \quad (12)$$

Protein adsorption tests can be used in order to evaluate the antifouling properties of membranes with bovine serum albumin (BSA) used in this case as a model foulant. Using the same apparatus as previously, the fouling of the membrane was also determined by adding a BSA aqueous solution (1 g L^{-1} in PBS, 0.1 M, pH = 7.0) in the hot feed. In order to evaluate the antifouling properties of membrane, the fouling ratio (R_f) was calculated every 15 min according to the following equation:

$$R_f = \left(1 - \frac{J}{J_0}\right) \times 100\% \quad (13)$$

where J is the flux of BSA solution after distillation at various times intervals (L m^{-2} h^{-1}) and J_0 is the initial flux of BSA solution at the beginning of the batch test (L m^{-2} h^{-1}).

3. Results & discussion

3.1 Characterization of SiF-NPs

SEM, TEM and AFM micrographs (Fig. 1) of SiF-NPs reveal that the fluorinated silica particles have a plate-like morphology with a uniform size of about 30 nm and thickness of about 1.2–1.4 nm. EDS analysis of SEM micrographs reveals that the Si : O atomic ratio is 1 : 1.94 ± 0.4 and the C : F atomic ratio is 1 : 0.98 ± 0.5 corroborating the formation of SiO_2 and the presence of fluoroalkyl chains in the nanoplates.

3.2 Membrane morphology analysis

The morphology of pristine and modified PVDF–HFP membrane (*i.e.* top surfaces and cross sections) was also studied by SEM. Fig. 2 shows that the surface of pristine membrane has rough and symmetric structure with small pores of diameter less than 1 μm. SEM of the modified membrane shows that SiF-NPs covered completely and uniformly the porous surface of the membrane, forming a layer

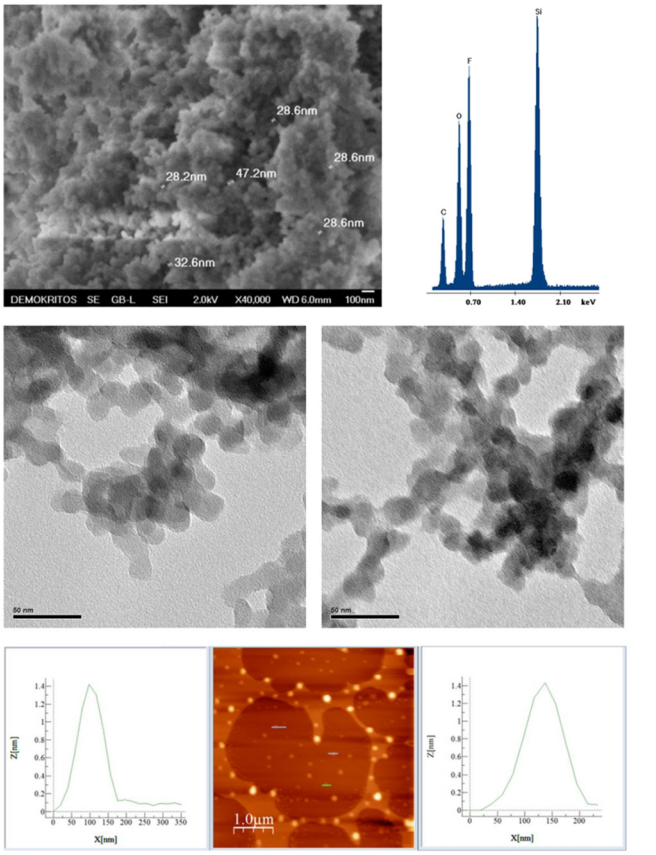

Fig. 1 First row: SEM microphotograph and EDS analysis of perfluorinated silicon oxide nanoparticles; second row: TEM images of nanoparticles; third row: AFM images and analysis of nanoparticles' height.

on the top membrane surface. The SiF-NPs on the PVDF–HFP membrane surface partially filled the pores, and thus slightly reduced the average pore size of the membrane. Also, the thickness of the pristine membrane was 60–65 μm, while the modified membrane was 75–80 μm, suggesting that the SiF-NPs layer is *ca.* 15 μm. The variation of the layer's thickness is expected to affect the membrane's performance. It is generally accepted that an increase of the membrane's thickness causes a reduction of the permeability,[24] while low thicknesses suffer generally from energy losses due to conductive heat flux. Extended research is required for the investigation of the optimum layer thickness.

3.3 TGA analysis

The TGA plots for SiF-NPs as well as for the pristine and modified PVDF–HFP membranes are shown in Fig. 3. It can be seen that both the SiF-NPs as well as the membranes exhibit excellent thermal stability up to 200 °C, while severe degradation is observed in the 400–600 °C temperature range. The residual weight at 800 °C was 30.74% for SiF-NPs, 16.14% for pristine and 17.55% for modified membrane, respectively. The content of SiF-NPs on the modified membrane is 9.1% wt. as calculated by the weight loss registered within the temperature range of 35–800 °C.

3.4 LEP, pore size, porosity & membrane surface wetting resistance analysis

In MD process, wetting resistance is the most significant parameter of any candidate membrane. When the membrane pores are dry, vapor occupies the empty void and separates the feed and distillate streams and prevents the passage of nonvolatile solutes. However, pore wetting does occur and is frequently associated with salt precipitation (scaling) on the membrane surface. Wetting resistance is based on the hydrophobicity and as it can be seen in Fig. 4 the water contact

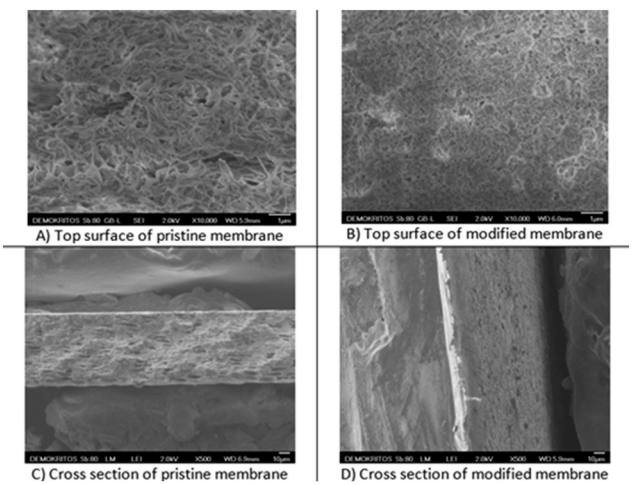

Fig. 2 SEM images of the top surface of the pristine and modified membranes (A and B respectively) and the corresponding cross section (C and D respectively).

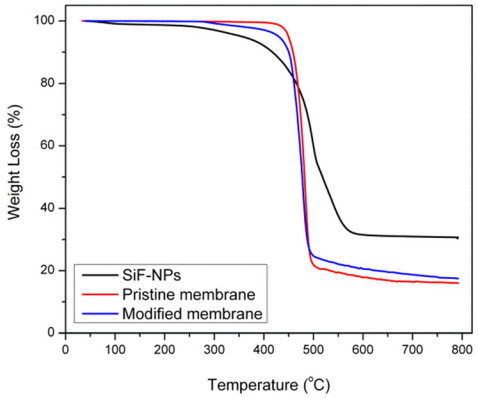

Fig. 3 The TGA curve of SiF-NPs, pristine PVDF–HFP and modified membrane.

angle (WCA) of the pristine membrane is relatively high ($\theta \approx 120°$). To enhance the wetting resistance of the membrane, a coating of superhydrophobic SiF-NPs was introduced on the surface of the membrane in order to become rougher and superhydrophobic ($\theta \approx 170°$). Furthermore, the calculation of SFE showed that the coating lowers significantly the SFE of the pristine membrane, from 5.46 to 0.3 mJ m^{-2}, due to fluorosilanization,[25] and consequently prevents membrane wetting. Therefore, as it was previously referred, water molecules have less direct contact with the membrane, due to the surface superhydrophobicity. Because of the low SFE, according to the eqn (4), the work of adhesion of the membrane is reduced from 5.5 to 0.4 mJ m^{-2}.

Membrane wetting resistance was also quantified by LEP, and it is assumed that if the transmembrane pressure exceeds the LEP, the feed will flood the membrane pores. As it can been seen in Table 1 the LEP of the pristine membrane is ≈2.7 bar, corresponding to a maximum pore radius ≈300 nm, while, as expected, the coating process did not significantly change the maximum pore size, resulting in LEP of 5.5 bar and a maximum pore radius of ≈265 nm. According to eqn (7), the effective mean pore size radius of pristine and modified membrane is 94 and 62 nm, respectively.

To determine the oleophobic properties of the membranes the following low surface tension organic compounds were used: octane (21.62 mN m^{-1}), dodecane (25.35 mN m^{-1}), methylnaphthalene (38.6 mN m^{-1}) and diidomethane (50.8 mN m^{-1}). The influence of the liquid surface tension on the

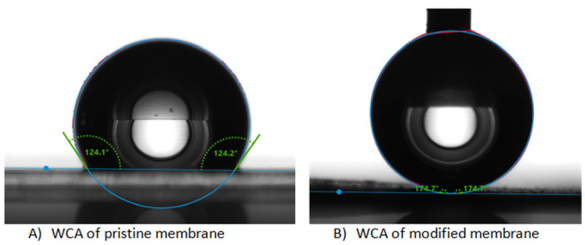

Fig. 4 Images of water contact angles of pristine (A) and modified membranes (B).

Table 1 Properties of the pristine PVDF–HFP and modified PVDF–HFP/SiF-NPs membranes

Membrane	PVDF–HFP (pristine)	PVDF–HFP/SiF-NPs (modified)
WCA (°)	124 ± 2	174 ± 3
LEP (bar)	2.7 ± 0.3	5.5 ± 0.2
$D_{max\text{-}LEP}$ (nm)	302 ± 16	264 ± 9
Porosity (%)	60 ± 5	58 ± 3

oleophobic properties is shown in Fig. 5. It is observed that the static contact angles slightly increase for lower surface tension liquids with the introduction of SiF-NPs layer on the membrane, while for the higher surface tension liquids the contact angle increase is much more profound. Thus, the liquid may be in a Wenzel state and the surface chemistry becomes predominant, which explains the increase in the contact angle due to the fluorinated groups.[26]

3.5 DCMD & fouling evaluation

Regarding the evaluation of the DCMD performance, the PVDF–HFP and modified PVDF–HFP/SiF-NPs membranes were tested using as feed NaCl solution (35 g L^{-1}) as model solution. The permeate flux of the pristine membrane was determined at 6 LMH, while the modified membrane had a flux of 17 LMH that is about 3 times higher. A possible explanation for this increase is that the addition of the non-wetting superhydrophobic particles layer alters the interface between water and polymeric matrix, increasing the vapor/membrane surface area[27] and reducing the temperature and concentration polarization.

In addition, according to eqn (10), the mass transfer resistance of pristine and modified membranes were determined as 0.59 and 1.64 × 10^{-7} kg m^{-2} s^{-1} Pa^{-1}, while according to eqn (11) 6.7 and 6.5 × 10^{-7}, respectevily. The salt rejection for both membranes was very effective and determined at a value above 99.98%. In order to study the fouling tendency of the membranes a BSA solution was used. Fig. 6 depicts the membrane performance under the 1 h BSA fouling test. It is evident that the flux of both membranes

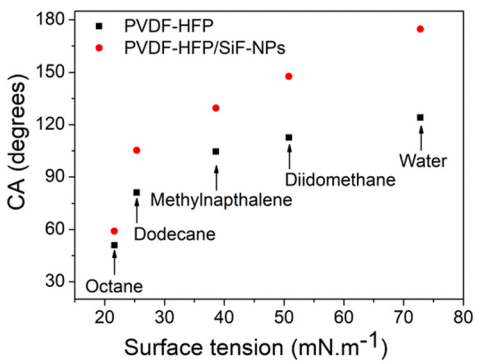

Fig. 5 Static contact angles as a function of the surface tension of apolar liquids on pristine and modified membranes.

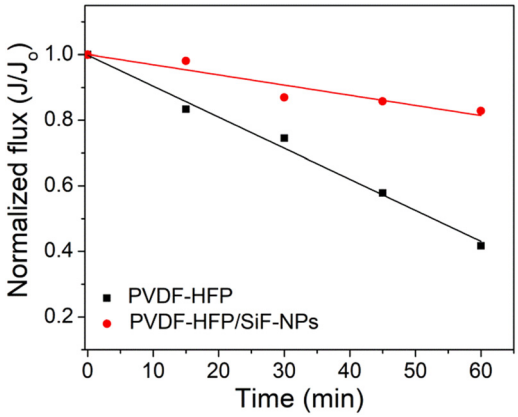

Fig. 6 Membrane performance in BSA fouling test-normalized flux (J/J_0) *vs.* time.

decreases upon time due to the pollutant layer formed by protein adsorption. However, it should be mentioned that the flux of the pristine membrane decreases 40% more than that of the modified nanocomposite membrane. Therefore, the R_f of the pristine membrane after 1 h is 58%, while that of SiF-NPs membrane is only 17%. These results suggest that the SiF-NPs on the surface of the membrane reduce substantially the fouling of the membrane, as they reduce the adsorption of organic substances onto hydrophobic PVDF–HFP surface.

The performance of the developed membranes was comparable to that of previous works, as shown in Table 2. The results are similar in terms of LEP, WCA and salt rejection, while the permeate flux of the other membranes vary. The membranes mentioned by the two literature sources are modified chemically, as opposed to the present research that provides a simpler methodology. Further research is necessary for the optimization of the membranes' performance. Additionally, membranes such as hydrophobic (PVDF, PTFE) or hyrdrophilic (PES), which are widely used in membrane distillation process[28–30] could be coated by SiF-NPs in order to estimate the compatibility of the coating with these membranes and to evaluate their perfomance.

The outlook of the present work is to establish an innovative technique of membrane preparation and modification *via* one-step method, in order to introduce non wetting characteristics, rendering membranes suitable for membrane distillation processes. The production of superhydrophobic membranes for MD system is of great importance due to the fact that current commercial hydrophobic membranes suffer from membrane wetting.

4. Conclusions

In summary, SiF-NPs were successfully prepared and applied as a coating in PVDF–HFP membranes. The characterization was conducted by various methods, while their performance in DCMD was evaluated. The experimental results showed that the application of a layer of superhydrophobic SiF-NPs

Table 2 Comparison of this work with previous research

Source	Type	LEP	WCA	Flux	Salt Rej.	Temp hot	Salt Conc.
—	—	Bar	°	LMH	%	°C	g L^{-1}
This work	PVDF–HFP/SiF-NPs	5.5	174	17	99.98	70	35
Zheng *et al.*[31]	PVDF–SiNPs@PS	4	176.5	9	99.8	60	10
Zhang *et al.*[32]	PVDF–SiNPs	5.5	169	37	99.9	70	35

had significant effects on the overall properties of the membrane. Specifically, DCMD experiments showed that the nanocomposite membrane had improved fouling resistance and increased permeability, retaining excellent salt rejection. Additionally, the wetting resistance against various liquids of low surface tensions was also enhanced compared to pristine PVDF–HFP membranes. The results indicate that the developed superhydrophobic membranes exhibit improved overall performance aiming to tackle critical issues of membrane distillation process.

Author contributions

Conceptualization, A. A. S. and D. T.; data curation, I. T., L. G. B., A. P. and N. K. B.; formal analysis, I. T., L. G. B., A. P. and N. K. B.; investigation, A. A. S., D. T. and Z. S.; methodology, I. T., L. G. B., A. P. and N. K. B.; project administration, A. A. S., D. T. and Z. S.; resources, A. A. S.; supervision, A. A. S. and D. T.; validation, A. A. S. and D. T.; visualization, A. A. S. and D. T.; writing – original draft, I. T., D. T. and Z. S.; writing – review and editing, A. A. S., D. T. and Z. S. All authors have read and agreed to the published version of the manuscript.

Conflicts of interest

The authors declare no competing financial interest.

Acknowledgements

This research was partially supported by European Union's Horizon 2020 research and innovation programme under grant agreement no. 958454, project intelWATT (Intelligent Water Treatment for water preservation combined with simultaneous energy production and material recovery in energy intensive industries) I. T. acknowledges financial support by the Hellenic Foundation for Research and Innovation (HFRI) under the 3rd Call for HFRI PhD Fellowships (Fellowship Number: 6628).

References

1 J. Yin and B. Deng, Polymer-matrix nanocomposite membranes for water treatment, *J. Membr. Sci.*, 2015, **479**, 256–275, DOI: **10.1016/j.memsci.2014.11.019**.
2 M. M. Pendergast and E. M. V. Hoek, A review of water treatment membrane nanotechnologies, *Energy Environ. Sci.*, 2011, **4**(6), 1946–1971.
3 Y. Yun, R. Ma, W. Zhang, A. G. Fane and J. Li, Direct contact membrane distillation mechanism for high concentration NaCl solutions, *Desalination*, 2006, **188**(1–3), 251–262.
4 J. Phattaranawik, R. Jiraratananon and A. G. Fane, Heat transport and membrane distillation coefficients in direct contact membrane distillation, *J. Membr. Sci.*, 2003, **212**(1–2), 177–193.
5 M. S. Islam, A. Sultana, A. H. M. Saadat, M. S. Islam, M. Shammi and M. K. Uddin, Desalination Technologies for Developing Countries: A Review, *J. Sci. Res.*, 2018, **10**(1), 77–97.
6 C. Meringolo, G. Di Profio, E. Curcio, E. Tocci, E. Drioli and E. Fontananova, State of the Art and Perspectives in Membranes for Membrane Distillation/Membrane Crystallization, in *Membrane Desalination*, CRS Press, New York, 2020, p. 125.
7 A. A. Sapalidis, Porous Polyvinyl alcohol membranes: Preparation methods and applications, *Symmetry*, 2020, **12**(6), 1–24.
8 D. Hou, H. Fan, Q. Jiang, J. Wang and X. Zhang, Preparation and characterization of PVDF flat-sheet membranes for direct contact membrane distillation, *Sep. Purif. Technol.*, 2014, **135**(1), 211–222, DOI: **10.1016/j.seppur.2014.08.023**.
9 J. E. Efome, M. Baghbanzadeh, D. Rana, T. Matsuura and C. Q. Lan, Effects of superhydrophobic SiO2 nanoparticles on the performance of PVDF flat sheet membranes for vacuum membrane distillation, *Desalination*, 2015, **373**, 47–57, DOI: **10.1016/j.desal.2015.07.002**.
10 W. Zhang, Y. Lu, J. Liu, X. Li, B. Li and S. Wang, Preparation of re-entrant and anti-fouling PVDF composite membrane with omniphobicity for membrane distillation, *J. Membr. Sci.*, 2019, 117563, DOI: **10.1016/j.memsci.2019.117563**.
11 R. Zheng, Y. Chen, J. Wang, J. Song, X. Li and T. He, Preparation of omniphobic PVDF membrane with hierarchical structure for treating saline oily wastewater using direct contact membrane distillation, *J. Membr. Sci.*, 2018, **555**, 197–205, DOI: **10.1016/j.memsci.2018.03.041**.
12 M. Arkas and D. Tsiourvas, Organic/inorganic hybrid nanospheres based on hyperbranched poly(ethylene imine) encapsulated into silica for the sorption of toxic metal ions and polycyclic aromatic hydrocarbons from water, *J. Hazard. Mater.*, 2009, **170**(1), 35–42.
13 C. Kyrou, D. Tsiourvas, S. Kralj and I. Lelidis, Effect of superhydrophobic nanoplatelets on the phase behaviour of liquid crystals, *J. Mol. Liq.*, 2020, **298**, 111984, DOI: **10.1016/j.molliq.2019.111984**.
14 W. Pu, X. He, L. Wang, C. Jiang and C. Wan, Preparation of PVDF–HFP microporous membrane for

Li-ion batteries by phase inversion, *J. Membr. Sci.*, 2006, **272**(1–2), 11–14.

15 J. M. Schuster, C. E. Schvezov and M. R. Rosenberger, Analysis of the Results of Surface Free Energy Measurement of Ti6Al4V by Different Methods, *Procedia Mater. Sci.*, 2015, **8**, 732–741, DOI: **10.1016/j.mspro.2015.04.130**.

16 Y. Xiu, L. Zhu, D. W. Hess and C. P. Wong, Relationship between Work of Adhesion and Contact Angle Hysteresis on Superhydrophobic Surfaces, *J. Phys. Chem. C*, 2008, 11403–11407, DOI: **10.1021/jp711571k**.

17 G. Rácz, S. Kerker, Z. Kovács, G. Vatai, M. Ebrahimi and P. Czermak, Theoretical and experimental approaches of liquid entry pressure determination in membrane distillation processes, *Period. Polytech., Chem. Eng.*, 2014, **58**(2), 81–91.

18 F. E. Ahmed, B. S. Lalia and R. Hashaikeh, Membrane-based detection of wetting phenomenon in direct contact membrane distillation, *J. Membr. Sci.*, 2017, **535**, 89–93, DOI: **10.1016/j.memsci.2017.04.035**.

19 C. Athanasekou, A. Sapalidis, I. Katris, E. Savopoulou, K. Beltsios and T. Tsoufis, *et al.*, Mixed Matrix PVDF/Graphene and Composite-Skin PVDF/Graphene Oxide Membranes Applied in Membrane Distillation, *Polym. Eng. Sci.*, 2019, **59**, E262–E278.

20 C. Feng, B. Shi, G. Li and Y. Wu, Preparation and properties of microporous membrane from for membrane distillation, *J. Membr. Sci.*, 2004, **237**, 15–24.

21 A. M. Alklaibi and N. Lior, Heat and mass transfer resistance analysis of membrane distillation, *J. Membr. Sci.*, 2006, **282**, 362–369.

22 K. Xin, I. Roghair, F. Gallucci and M. van Sint Annaland, Total vapor pressure of hydrophobic deep eutectic solvents: Experiments and modelling, *J. Mol. Liq.*, 2021, **325**, 115227, DOI: **10.1016/j.molliq.2020.115227**.

23 J. Phattaranawik, R. Jiraratananon and A. G. Fane, Effect of pore size distribution and air flux on mass transport in direct contact membrane distillation, *J. Membr. Sci.*, 2003, **215**(1–2), 75–85.

24 E. Drioli, A. Ali and F. Macedonio, Membrane distillation: Recent developments and perspectives, *Desalination*, 2015, **356**, 56–84, DOI: **10.1016/j.desal.2014.10.028**.

25 A. Razmjou, E. Arifin, G. Dong, J. Mansouri and V. Chen, Superhydrophobic modification of TiO 2 nanocomposite PVDF membranes for applications in membrane distillation, *J. Membr. Sci.*, 2012, **415–416**, 850–863, DOI: **10.1016/j.memsci.2012.06.004**.

26 H. Bellanger, T. Darmanin and F. Guittard, Surface structuration(micro and/or nano) governed by the fluorinated tail lengths toward superoleophobic surfaces, *Langmuir*, 2012, **28**(1), 186–192.

27 H. Shan, J. Liu, X. Li, Y. Li, F. H. Tezel and B. Li, *et al.*, Nanocoated amphiphobic membrane for flux enhancement and comprehensive anti-fouling performance in direct contact membrane distillation, *J. Membr. Sci.*, 2018, **567**, 166–180.

28 C. Meringolo, T. F. Mastropietro, T. Poerio, E. Fontananova, G. De Filpo and E. Curcio, *et al.*, Tailoring PVDF Membranes Surface Topography and Hydrophobicity by a Sustainable Two-Steps Phase Separation Process, *ACS Sustainable Chem. Eng.*, 2018, **6**(8), 10069–10077.

29 H. J. Hwang, K. He, S. Gray, J. Zhang and I. S. Moon, Direct contact membrane distillation(DCMD): Experimental study on the commercial PTFE membrane and modeling, *J. Membr. Sci.*, 2011, **371**(1–2), 90–98.

30 S. Ghorabi, F. Z. Ashtiani, M. Karimi, A. Fouladitajar, B. Yousefi and F. Dorkalam, Development of a novel dual-bioinspired method for synthesis of a hydrophobic/hydrophilic polyethersulfone coated membrane for membrane distillation, *Desalination*, 2021, **517**, 115242, DOI: **10.1016/j.desal.2021.115242**.

31 R. Zheng, Y. Chen, J. Wang, J. Song, X. Li and T. He, Preparation of omniphobic PVDF membrane with hierarchical structure for treating saline oily wastewater using direct contact membrane distillation, *J. Membr. Sci.*, 2018, **555**, 197–205.

32 W. Zhang, Y. Lu, J. Liu, X. Li, B. Li and S. Wang, Preparation of re-entrant and anti-fouling PVDF composite membrane with omniphobicity for membrane distillation, *J. Membr. Sci.*, 2019, 117563.